

Whales At the Crossroads: Soundscape Dynamics, Movement Ecology, and Conservation Implications for Southern Resident Killer Whales in the Waters off Rum Island in the Salish Sea

Mathias POULY^{1,2}

¹Master's in Ecophysiology, Ecology, and Ethology, Faculty of Life Sciences, University of
Strasbourg

²School of Environmental Science, Simon Fraser University



August 15, 2025



QENTOL, YEN
WSÁNEĆ Marine Guardians

Student: Mathias Pouly

Master: Ecology, Ecophysiology, Ethology

Host laboratory: School of Environmental Science, Simon Fraser university

Supervisor: Dr Ruth Joy (rjoy@sfu.ca)

Title: Whales at the Crossroads: Soundscape Dynamics, Movement Dynamics, and Conservation Implications for Southern Resident Killer Whales in the Waters off Rum Island

Keyword: Underwater noise pollution, Southern resident killer whales, Soundscape dynamic, Vessel traffic, Hydrodynamics, Movement trajectories, Passive acoustic monitoring

Abstract

Understanding how endangered marine mammals adjust their movements and trajectories in response to environmental and anthropogenic pressures is crucial for conservation. In the Salish Sea, Southern Resident Killer Whales (SRKW; *Orcinus orca*) navigate through a complex network of archipelagos, islands, and channels subject to high hydrodynamic variability and persistent acoustic pressure caused by intense maritime traffic. This study investigates SRKW routing decisions at a key spatial junction near Rum Island, where three major corridors, Haro Strait, Swanson Channel, and Boundary Pass, converge. The local soundscape was first characterized, and 69 SRKW trajectories were reconstructed from combined visual and acoustic detections. These were modeled using a multinomial generalized additive model (GAM) in relation to broadband sound pressure levels (SPL), surface current speed, and direction. Descriptive soundscape analysis confirmed the predominance of anthropogenic noise from vessel traffic, with strong temporal variability driven by abiotic factors and shipping activity, and measurable reductions associated with vessel slowdown measures. In the multinomial model, only variables related to current significantly influenced route selection: the probability of using Haro Strait increased with stronger southwesterly currents, consistent with energy-efficient use of ebb tidal flows. While broadband SPL was not a statistically significant predictor, a consistent, non-significant trend toward Swanson Channel under higher noise conditions suggests a potential behavioural sensitivity to acoustic disturbance. These findings identify Rum Island as a critical decision point, where routing through different corridors reflects a multi-criteria navigation strategy shaped by hydrodynamics conditions and acoustic exposure. These highlight the need for long-term, fine-scale monitoring that integrates biologically weighted acoustic metrics, foraging opportunities, and social factors to better understand the ecological trade-offs underlying corridor selection. Implementing targeted noise-reduction measures in such decision-critical areas could help maintain functional connectivity among essential habitats and strengthen the resilience of this population.

Abbreviation used:

- **SRKW** – Southern Resident Killer Whales
- **DFO** – Department of Fisheries and Oceans
- **NMFS** – National Marine Fisheries Service
- **PAM** – Passive Acoustic Monitoring
- **BCHN** – British Columbia Hydrophone Network
- **IC-LISTEN** – Intelligent Compact LISTENing hydrophone
- **AIS** – Automatic Identification System
- **ERDDAP** – Environmental Research Division’s Data Access Program
- **FLAC** – Free Lossless Audio Codec
- **PSD** – Power Spectral Density
- **SPL** – Sound Pressure Level
- **dB re 1 μ Pa** – Decibel relative to 1 microPascal
- **μ Pa** – Micropascal (unit of pressure)
- **Hz** – Hertz (unit of frequency)
- **$L_{p,i}$** – Received Sound Pressure Level from vessel i **LS_i** – Source Level of vessel i
- **$L_{p,sum}$** – Cumulative Received Sound Pressure Level from vessels
- **ACF** – Autocorrelation Function
- **GAM** – Generalized Additive Model
- **EDF** – Estimated Degrees of Freedom
- **AIC** – Akaike Information Criterion
- **RMS** – Root Mean Square
- **ECHO** – Enhancing Cetacean Habitat and Observation Program
- **r_s** – Spearman’s rank correlation coefficient
- **p or p -val** – Probability value (p-value)
- **m/s** – Meters per second (unit of current speed)
- **L95** – 95th percentile sound pressure level
- **SEL** – Sound Exposure Level

Participation of the student

- **Data collection:** 0 %
- **Data treatment:** 99 %
- **Statistical analysis:** 100 %
- **Report writing:** 99 %

Acknowledgment

I would like to begin by expressing my deepest gratitude to Ruth Joy, for her kindness, generosity with her time, and exceptional expertise. I am profoundly thankful for the remarkable opportunity she gave me to immerse myself in this captivating field of research. Under her guidance, I was able to learn so much, not only about science, but also about the value of curiosity, perseverance, and collaboration. This experience allowed me to witness unforgettable moments alongside marine mammals in one of the most beautiful regions of North America, memories that will stay with me forever. I am also deeply thankful to the WSÁNEĆ Marine Guardians for providing me invaluable data, welcoming me into their world and allowing me to accompany them in the field. Being able to follow and observe their work firsthand was a privilege, and their dedication to protecting the species and habitats of these waters continues to fascinate and inspire me. Their research initiatives, coupled with their profound knowledge of Salish Sea ecosystems, were essential for collecting the invaluable data from Rum Island that forms the foundation of this work. My gratitude also extends to those I had the chance to meet and collaborate with during this journey, such as Kaitlin Palmer, Benjamin Hendricks, Dylan Smyth, Peter Thompson, and the Ocean Wise team, each of whom generously contributed pieces of knowledge, skills, and precious data that broadened my perspective and enriched this project far beyond what I initially imagined possible. I would also like to warmly thank my lab friends, including Cassandra, Saniya, Dylan, and Andrea, whose support, camaraderie, and humor made the work environment not only productive but also joyful. Finally, I am endlessly grateful to my family and friends, who have been my unwavering source of emotional support, despite the nine-hour time difference. Their encouragement, patience, and belief in me have been the anchor that carried me through every challenge.

Summary

Introduction.....	1
Material and methods.....	3
1. Descriptive analysis of Rum Island Soundscape.....	4
1.1. Acoustic Data Collection	4
1.1. Acoustic Data Processing.....	5
1.2. Navigation and Environmental variables	5
1.3. Descriptive statistics	6
2. Influence of soundscape and environment on SRKW trajectories.....	7
2.1. Acquisition of Orca Observation Data.....	7
2.2. Definition and Extraction of SRKW Trajectories.....	7
2.3. Explanatory variables.....	8
2.4. Statistical model.....	9
Results	10
1. Descriptive analysis of Rum Island Soundscape.....	10
1.1. Environmental variables and soundscape	10
1.2. Shipping traffic and soundscape	11
2. Influence of soundscape and environment on SRKW trajectories.....	12
2.1. Trajectory distribution.....	12
2.2. Statistical model results	12
Discussion	14
1. Soundscape at Rum Island: a noisy crossroad?	14
2. Routes adjustment to sound and currents	16
Conclusion.....	20
Bibliography	21

Introduction

Coastal marine habitats are increasingly shaped and disrupted by human activities. These industrial activities degrade the habitat's ecological quality but also disrupt the distribution and behaviours of the species that depend on them. Among stressors, underwater noise pollution stands out as a particularly dangerous form of disturbance. Although invisible, it is now a pervasive threat across the world's oceans, due to the ongoing expansion of maritime traffic. Since the 1950s, global ambient noise levels have risen by an estimated 3.3 dB, a trend projected to intensify in the coming decades (Frisk, 2012).

In marine environments, anthropogenic noise has become a dominant component, altering the acoustic conditions, and disrupting species communication and behaviour. Given the limited visibility in underwater environments, many marine species, including toothed whales, depend on acoustic cues to navigate, locate prey, and maintain social bonds (Erbe et al. 2018). For these marine mammals, noise pollution can interfere with communication, impair foraging efficiency, and fragment social cohesion. Chronic exposure may even displace whales driving them away from critical habitats (Williams et al. 2006).

Among the most critically affected populations are the Southern Resident killer whales (*Orcinus orca*) (SRKW), an endangered killer whale population endemic to the northeastern Pacific Ocean, particularly the Salish Sea (Canada species at Risk Act, 2002). This population of resident ecotype killer whales consists of three matrilineal pods, J, K, and L, with an estimated 73 individuals remaining as of 2023, reflecting a long-term decline from 99 individuals in the mid-1990s (Murray et al. 2019). SRKW are characterized by strong social bonds, with individuals remaining in their natal pod throughout their lives and a strong dietary dependence on Chinook salmon (*Oncorhynchus tshawytscha*) stocks, also in decline (Ford et al. 2017). As such, their survival is challenged by compounding anthropogenic threats, including declining Chinook stocks due to habitat degradation and climate change, bioaccumulation of chemical contaminants, and pervasive underwater noise.

The Salish Sea is one of the most acoustically polluted regions in the world, driven by the high density of maritime traffic from major commercial hubs like Vancouver, Seattle, and Tacoma (Erbe et al. 2012). Large commercial vessels, such as container ships and bulk carriers, generate low-frequency noise (typically <10 kHz), raising sound pressure levels (SPL) by up to over 20 dB re 1 μ Pa (Veirs & Veirs, 2016). In addition, recreational boats, though smaller in size, contribute significantly to mid- and high-frequency noise, complicating mitigation efforts due to their unregulated movements and lack of mandatory tracking (Erbe et al. 2012).

This acoustic pollution within the core habitat of the SRKW disrupts their behaviour through both direct and indirect pathways. Documented impacts include masking of communication and echolocation, reduced foraging efficiency through altered time-activity budgets, and compromised social interactions (Erbe et al. 2018; Veirs & Veirs, 2016). Chronic exposure to high noise may also trigger physiological stress responses such as hearing loss or stress hormone production, further exacerbating the vulnerability of this fragile population (Holt, 2008). In response, initiatives such as Vancouver's ECHO Program have established voluntary vessel slowdown zones since 2019, which have shown measurable reductions in broadband noise levels and improvements in SRKW foraging behaviour, as well as an interim sanctuary zone implemented by Transport Canada that prohibit the passage of any boat into it (Fisheries and Oceans Canada. (2025)).

Beyond immediate disruptions, growing evidence suggests that acoustic pollution may reshape how SRKW use space, including movement patterns through critical habitats (Williams & Ashe, 2007). However, navigation decisions in these habitats are not determined solely by anthropogenic factors. The Salish Sea features highly dynamic hydrodynamics conditions, with spatial and temporal variations in current patterns driven by tides, topography, and freshwater inflows from rivers. These hydrodynamics interact with biological drivers such as prey availability that shape marine mammals' routing behaviour by balancing energetics costs and foraging availability (Gibson, 2003). While their distribution is primarily structured around the abundance and availability of Chinook salmon, key foraging areas often overlap with intense vessel activity simultaneously exposing whales to elevated noise exposure. Haro Strait and Boundary Pass, two of the most important feeding grounds, have been designated as critical habitats (DFO, 2017), yet they also coincide with some of the busiest shipping lanes in the region, particularly from traffic bound for the Port of Vancouver. This creates an ecological trade-off between essential ecological functions and anthropogenic disturbance. Despite these pressures, SRKW continue to frequent these corridors, especially along the west coast of San Juan Island during summer months (Olson et al. 2018), highlighting the complex interplay between hydrodynamic variability, foraging opportunity, and acoustic costs in their movement.

Within the Salish Sea, SRKW frequent waters adjacent to the southern Gulf Islands and northern San Juan Islands, particularly through the Haro Strait-Boundary Pass and Swanson Channel corridors. However, contrary to Haro Strait and Boundary Pass, Swanson Channel experiences significantly lower commercial vessel traffic due to its absence of direct port connections. These routes have historically been used continuously by SRKW throughout past decades with J pod present year-round, and K and L pods returning seasonally to these corridors each summer. Haro

Strait is a high-use corridor shared by all pods (Hauser et al. 2007; Olson et al. 2018), however, precise reconstructions of their movement trajectories through these three corridors, and the factors influencing routing decisions remain poorly understood. While cultural transmission likely shapes these whales' movement, the roles of anthropogenic pressures and hydrodynamics conditions are also likely to influence their movement patterns.

In this context, Rum Island stands out as a particularly interesting area for studying SRKW movement ecology. Located at the confluence of Haro Strait, Boundary Pass, and Swanson Channel, it forms a strategic junction where whales repeatedly make routing decisions toward one of three corridors. This area combines intense vessel traffic with highly variable hydrodynamics conditions, as tidal flows differ in strength and direction across corridors depending on the relative position with rivers and oceans. Its central position offers an opportunity to examine how maritime noise and physical oceanography shape local soundscapes and influence whale movement patterns.

With the increasing integration of passive acoustic monitoring (PAM) and oceanographic data, it is becoming possible to explore how these whales respond to dynamic seascapes shaped by both anthropogenic and natural drivers. In this study, we focused on SRKW movements around Rum Island. The aim was twofold: First, we characterized the soundscape of Rum Island by quantifying the contributions of anthrophony and geophony, providing context to assess the use of a global soundscape metric as a proxy for acoustic disturbance. Second, we examined SRKW routes passing Rum Island and how these trajectories respond to both soundscape and hydrodynamic drivers.

Given Rum Island's central location, we hypothesize that vessel traffic is the primary driver of the local soundscape, particularly by increasing broadband noise levels in the low-frequency bands, while natural geophysical processes such as wind or precipitation are expected to dominate higher-frequency noise components. We further hypothesize that SRKW adjust their routing decisions in response to this acoustic environment, tending to avoid noisier corridors such as Boundary Pass or Haro Strait under elevated SPL conditions, potentially favoring the quieter Swanson Channel. In parallel, we expect hydrodynamics conditions to influence movement patterns, with whales more likely to transit through corridors with strong favorable currents, such as Haro Strait or Boundary Pass, thereby reducing energetic costs and aligning with prey availability. By establishing key ecological context around movement trajectories, this study provides a foundational framework for understanding the interplay between noise pollution, oceanographic conditions, and the spatial behaviour of this population within the Southern Gulfs Islands. It also lays the groundwork for more detailed acoustic analyses to better inform and refine conservation strategies in this critical habitat.

Material and methods

All data in this study span a nearly two-year period from September 9, 2023, to June 1, 2025, thereby allowing for the integration of seasonal variability in acoustic conditions, environmental parameters, and SRKW movement patterns.

1. Descriptive analysis of Rum Island Soundscape

1.1. Acoustic Data Collection

The Salish Sea is subject to a large-scale acoustic monitoring program based on a network of hydrophones deployed as part of a PAM program, known as the British Columbia Hydrophone Network (BCHN). It was established over the past decades with the shared goal of monitoring and recording marine mammal vocalizations, particularly those of the SRKW, to improve knowledge and support conservation. The acoustic data used in this study come from a hydrophone deployed in the Rum Island area (XELEXÁTEM) by the QENTOL, YEN Marine Guardians, a team of marine scientists who blend traditional ecological knowledge with modern scientific methods.

The PAM device used is an Ocean Sonics IC-LISTEN HF hydrophone, installed on a sedimentary seabed at 18 meters depth off the western coast of Rum Island (Fig.1). The hydrophone is oriented East/Northeast and can detect acoustic signals up to approximately 5 nautical miles. The hydrophone monitors the commercial shipping lanes and a high-traffic recreational boating region between Canada's southern Gulf Islands (including Rum Island) and the United States' San Juan Islands.

The mooring system was designed to minimize noise disturbances caused by hydrodynamic turbulence, water column movement, and direct contact with the substrate. The hydrophone is connected to a solar-powered surface unit, ensuring continuous energy autonomy and a telemetry system that enables remote monitoring of the equipment's operational status (Fig. 2). Despite these precautions, two extended recording interruptions in March 2024 and October 2024 occurred due to equipment failures. Continuous recordings were segmented into 5-minute files encoded in FLAC format with a 24-bit resolution and a sampling frequency of 64 kHz, providing acoustic coverage up to 25 kHz (Nyquist frequency).

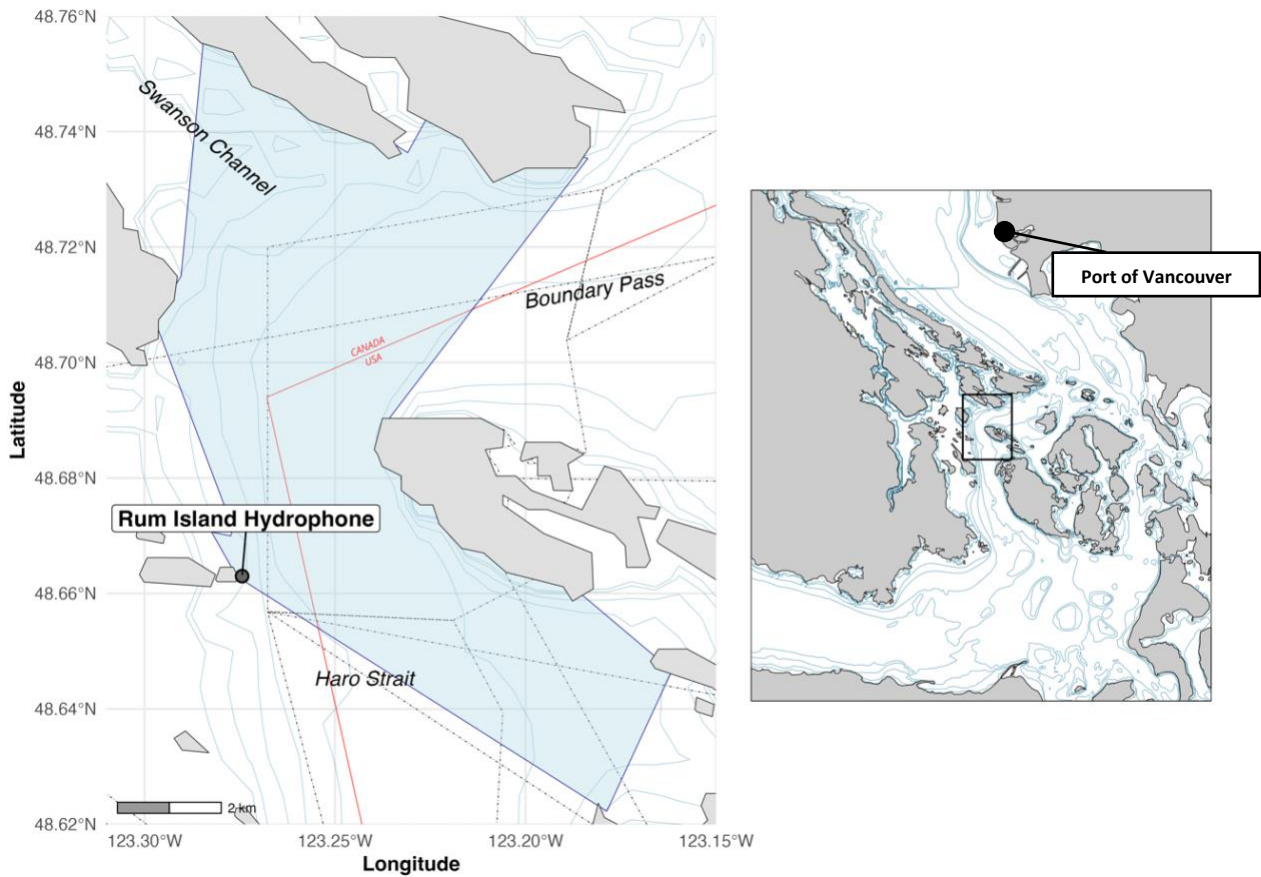


Figure 1. Left panel: Location of the Rum Island hydrophone within the Southern Gulf Islands, showing its estimated listening and whale detection range (blue polygon), adjacent commercial shipping lanes (dashed lines), bathymetry (blue line) and the Canada–USA maritime boundary (red line). Right panel: Broader overview of the Salish Sea, highlighting the geographic extent of the left panel (black square).



Figure 2. Photograph of the hydrophone deployment setup. Left: Monitoring system (black box) containing computer, battery; Right: Solar panel.

1.2. *Acoustic Data Processing*

The acoustic data processing was performed using custom Python scripts ([GitHub repository](#)). For each 5-minute recording, we calculated the power spectral density (PSD) root mean square (rms) using Welch's method, applying a 1-second Hanning window with 50% overlap. This ensured a frequency resolution of 1 Hz. Spectral levels were corrected based on the hydrophone sensitivity, with linear interpolation of the calibration curves (average sensitivity = -177.2 dB re 1 μ Pa). Finally, PSD values were converted into root-mean-square sound pressure levels (SPL) referenced to 1 μ Pa in the marine environment using the standard logarithmic relationship.

SPL values were calculated in one-third-octave bands ranging from 10 Hz to 25 kHz, however, low-frequency interference affected the data between 10 and 100 Hz from September 10, 2023, to March 4, 2024. As a result, third-octave bands within this range were excluded from statistical analyses to avoid bias. Additionally, SPL source-specific bands were extracted based on the characteristic spectral signatures of each noise contributor (see Table 1).

1.3. *Navigation and Environmental variables*

To characterize the anthropogenic and environmental contributions to the local soundscape, we integrated data on vessel activity and environmental conditions over the detection range of the Rum Island hydrophone. Vessel movements within the listening range were obtained through the Automatic Identification System (AIS) from the AccessAIS website, enabling the identification and classification of every commercial vessel transiting past Rum Island.

To robustly quantify the acoustic impact of shipping traffic, we computed an integrative metric to represent the cumulative sound exposure of all vessels detected near the hydrophone (Fig. 3) from Basan et al. 2024. For each vessel i , the received level $L_{p,i}$ at the hydrophone was first calculated from its source sound level $L_{S,i}$, which was estimated based on its category using values from (JASCO, 2014), and its distance to the hydrophone r_i using a spherical spreading loss formula adapted to the marine environment:

$$L_{p,i} = L_{S,i} - \left(A + B \cdot \log_{10} \left(\frac{r_i}{r_0} \right) \right) \text{ dB}, \quad \text{with } r_0 = 1 \text{ m}$$

The cumulative received level $L_{p,sum}$ from all commercial vessels passing was calculated for each time step chosen depending on autocorrelation test.

	Band (Hz)	Description
Vessel	100-1000 Hz	Vessel presence marker
Vessel	57-71 Hz	63 1/3 octave band
Vessel	113-141 Hz	125 1/3 octave band
Abiotic	10-100 Hz	Low-frequency wind, wave, and water turbulence
Abiotic	7500-8500 Hz	Wind speed
Abiotic	19500-20500 Hz	Precipitation noise
Soundscape	10-25000 Hz	Broadband acoustic soundscape

Table 1. Spectral bands used for soundscape analysis and their associated sources. Frequency bands (in Hz) corresponding to specific noise contributors, including vessel noise, abiotic factors (wind, precipitation), and broadband soundscape metrics (Vagle et al. 2021)

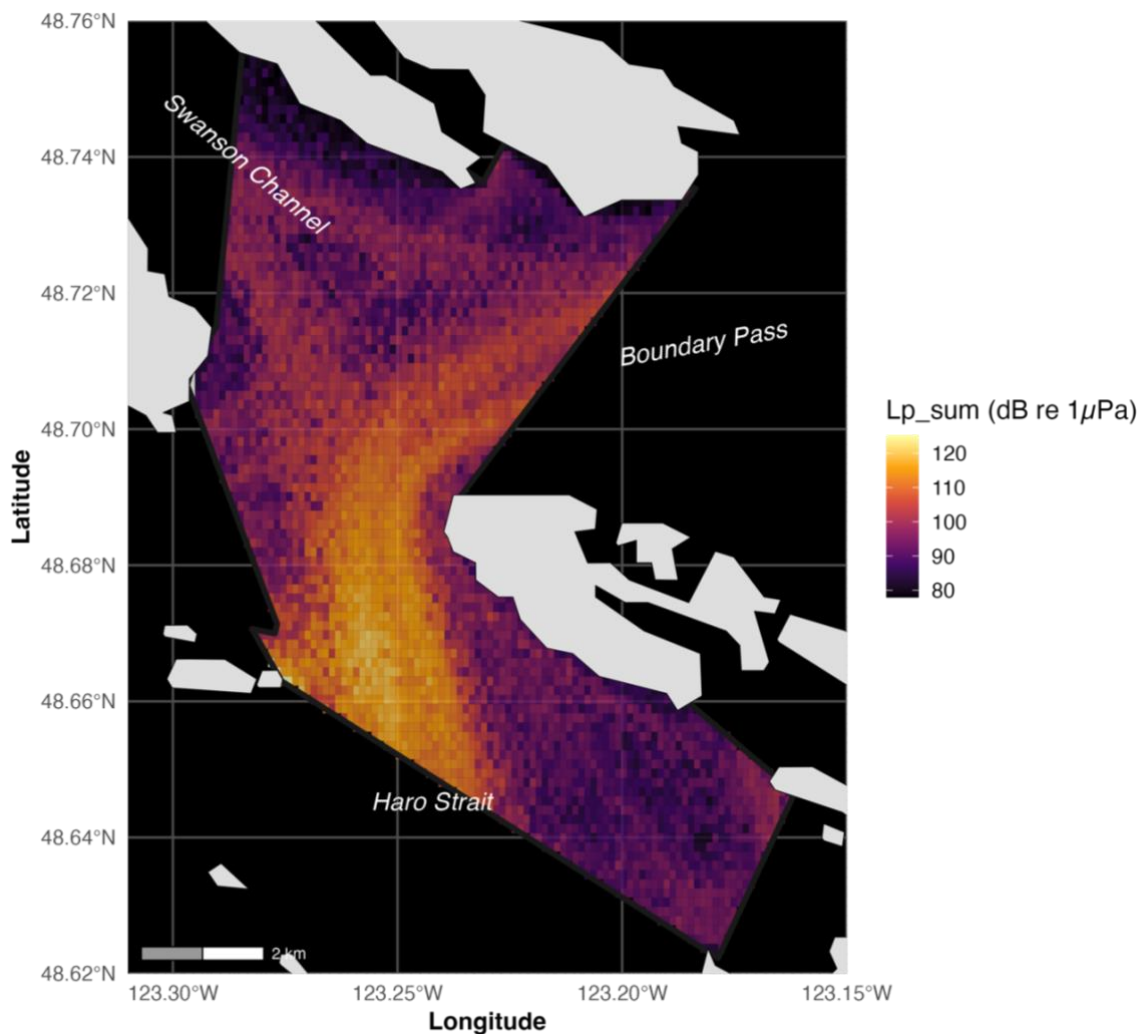


Figure 3. Mapping of $L_{p,sum}$ metrics calculated from AIS data, with each pixel representing the cumulative $L_{p,sum}$ value for that location over the period from March 9, 2023, to June 1, 2025. This visualization highlights major commercial shipping routes and their hypothetical impact on the soundscape recorded by the hydrophone.

The cumulative sound exposure was then computed using the standard logarithmic energy addition method:

$$L_{p,sum} = 10 \cdot \log_{10} \left(\sum_{i=1}^N 10^{L_{p,i}/10} \right) \text{ dB}$$

This metric was calculated both for all vessels combined, and separately for each vessel category. The categories considered included cargo ships, tankers, recreational boats, passenger vessels, tugboats, and fishing boats.

In parallel, key dynamic environmental variables known to influence the soundscape were extracted from the SalishSeaCast ERDDAP system (Soontiens et al. 2017). SalishSeaCast is a three-dimensional physical-biological-chemical ocean model that covers the Canadian and U.S. waters of the Salish Sea, providing estimates of wind speed, precipitation, and current velocity at 18-meter depth, matching the hydrophone deployment depth at Rum Island.

1.4. Soundscape statistics

1.4.1. Effects of variables on third-octave SPL

We analyzed soundscape composition using a non-parametric Spearman correlation test to evaluate frequency-specific relationships between SPL of each third-octave band and key variables including wind, rainfall, current speed and cumulative ship received level ($L_{p,sum}$). To mitigate autocorrelation, we first determined the optimal time lag between acoustic samples ensuring avoidance of autocorrelation in the Spearman coefficients. For ship correlations, SPL values were averaged over 15-minute intervals to match the temporal resolution of the $L_{p,sum}$ calculation and to reduce autocorrelation, whereas environmental variables were averaged over one-hour intervals.

1.4.2. SPL temporal comparison test

To evaluate seasonal SPL variations across frequency bands, we performed Kruskal-Wallis tests. These tests compared seasonal differences (winter vs. summer) within each environmental and vessel frequency band. For vessel-related frequency bands, SPL were also compared between periods with (June 1 to Nov 30) and without (Dec 1 to May 31) mandatory vessel speed reductions. To isolate the effect of speed restrictions and minimize environmental variability, analyses were grouped according by lunar phase, including only recordings when a vessel was detected within 5 km of the hydrophone. Medians (50th), and 5th–95th percentiles illustrated SPL distribution and variability were calculated for each comparison to assess background noise level and rare, intense noise events.

2. Influence of soundscape and environment on SRKW trajectories

2.1. *Acquisition of Orca Observation Data*

To connect SRKW observations into pod trajectories, acoustic and visual detections were combined. Acoustic detections were obtained through an automatic detection algorithm developed by Benjamin Hendricks (Sound Space Analytics) detections performed on the entire Rum Island dataset, along with manual detections performed on this dataset too as well as other hydrophone datasets such as Lime kiln hydrophone (Haro Strait) and East point hydrophone (Boundary Pass). Second, visual observations from citizen science networks were provided by two nongovernmental organizations, Oceanwise (Canada) and Acartia (USA) including observations from research campaigns and citizen scientists.

2.2. *Definition and Extraction of SRKW Trajectories*

Acoustic and visual observations of SRKW were combined to reconstruct realistic movement trajectories across the different corridors surrounding Rum Island. These zones were defined based on the detection range of the Rum Island hydrophone, encompassing Haro Strait to the south, Boundary Pass to the northeast, and Swanson Channel to the northwest (Fig. 4).

Given that SRKW pods can be spread across large areas and individual sightings may represent only part of a group, simply connecting observations in chronological order often results in inaccurate and disordered trajectories. To address this, we applied a filtering method based on Lin et al, 2025 in which two consecutive sightings were included in the same trajectory only if they occurred within two hours of each other and the distance between them implied a travel speed not exceeding 30 km/h. Trajectories were discarded if they did not pass through the Rum Island detection zone, and isolated points were excluded.

Spatio-temporal interpolation was then performed between each pair of consecutive points to represent the continuous movement of individuals. A transition matrix was built from a raster of the study area using the PBSmapping R package, to constrain movements within the ocean, excluding land areas. A Dijkstra Shortest Path algorithm was then applied to generate a regular spatial interpolation between each pair of consecutive points for each trajectory. Timestamps were interpolated proportionally to the relative spatial position and the time interval between observations. This method ensured ecological plausibility and maximized meaningful movement patterns, providing a solid foundation for subsequent modeling

2.3. Explanatory variables

We selected a single acoustic broadband SPL metric (100-25,000 Hz) as our soundscape variable describing Rum Island; this avoided the issue of multicollinearity from multiple frequency-specific SPL measures (Table.1). The 100-25,000 Hz frequency range captures the dominant spectral components of anthropogenic noise, environmental sounds, as well as SRKW vocalizations, including calls and, to some extent, echolocation clicks. This frequency range is considered a robust proxy to assess behavioural disturbance in SRKW (Heise et al. 2017) and captures key acoustic patterns while reducing complexity in the model without compromising ecological meaning or scientific standards. To account for vessel traffic intensity, we derived a ship density metric representing the number of vessels within a 5 km radius window (from AIS data) around each acoustic detection.

Finally, hydrodynamic variables were extracted from the SalishSeaCast ERDDAP database and include surface current vectors (direction and speed) calculated from the *u* (east-west) and *v* (north-south) velocity components of the surface currents. These variables were selected because of their potential to influence short-term movement decisions by SRKW where dynamic tidal processes affect current patterns relevant for modeling movement decisions.

We spatially and temporally aligned each variable to the corresponding point along the SRKW trajectories, based on the precise time and location of each point. For hydrodynamic variables (surface current speed and direction), the mean value for each trajectory was calculated by averaging across all associated points of the trajectories. To assess anthropogenic pressure specifically within the waters of Rum Island, we focused only on the broadband SPL and vessel presence variables. These were extracted and averaged exclusively over the subset of trajectory points that occurred within the spatio-temporal window corresponding to the SRKW passage through Rum Island. This distinction ensures that anthropogenic metrics reflect only the localized exposure encountered during transit through Rum Island.

2.4. Statistical model

We analyzed SRKW movement decisions near Rum Island using a multinomial generalized additive model (GAM) using the *mgcv* package on Rstudio, predicting probabilities of three route direction probabilities: Boundary Pass, Swanson Channel and Haro Strait (Fig.4). This model framework accommodated these three categorical outcomes describing route direction outcomes, while allowing for nonlinear effects of a set of covariates using smooth functions. This approach linked habitat variables to movement outcomes that are a function of whale directional choices. Trajectories were categorized by their destination rather than their origin, to better reflect the role of Rum Island as a decision point where whales select their route.

As a result, the model estimates the log-odds of selecting either Haro Strait or Swanson Channel relative to Boundary Pass (the reference level), with smooth spline functions representing nonlinear effects of each predictor on the log-odds of each directional choice. Boundary Pass was chosen as the reference level because this trajectory involves fewer assumptions and predictions about influencing factors compared to the other two routes, making it a more neutral baseline for comparison. Smooth splines were applied to all predictor variables, including broadband SPL, to capture potential non-linearities such as threshold effects or saturation. Given the circular nature of current directions, a cyclic cubic spline was used to ensure continuity at the 0–360° range. A month variable was also included to account for potential seasonal patterns and reduce autocorrelation.

The predicted probabilities for each direction were computed based on the fitted model. For every combination of variable values, the models create a linear score for each category which is then transformed into a probability using the SoftMax function. This approach allows to estimate, for any given set of variables, the predicted probability of occurrence for each response category, ensuring that they are mutually dependent and always sum to one.

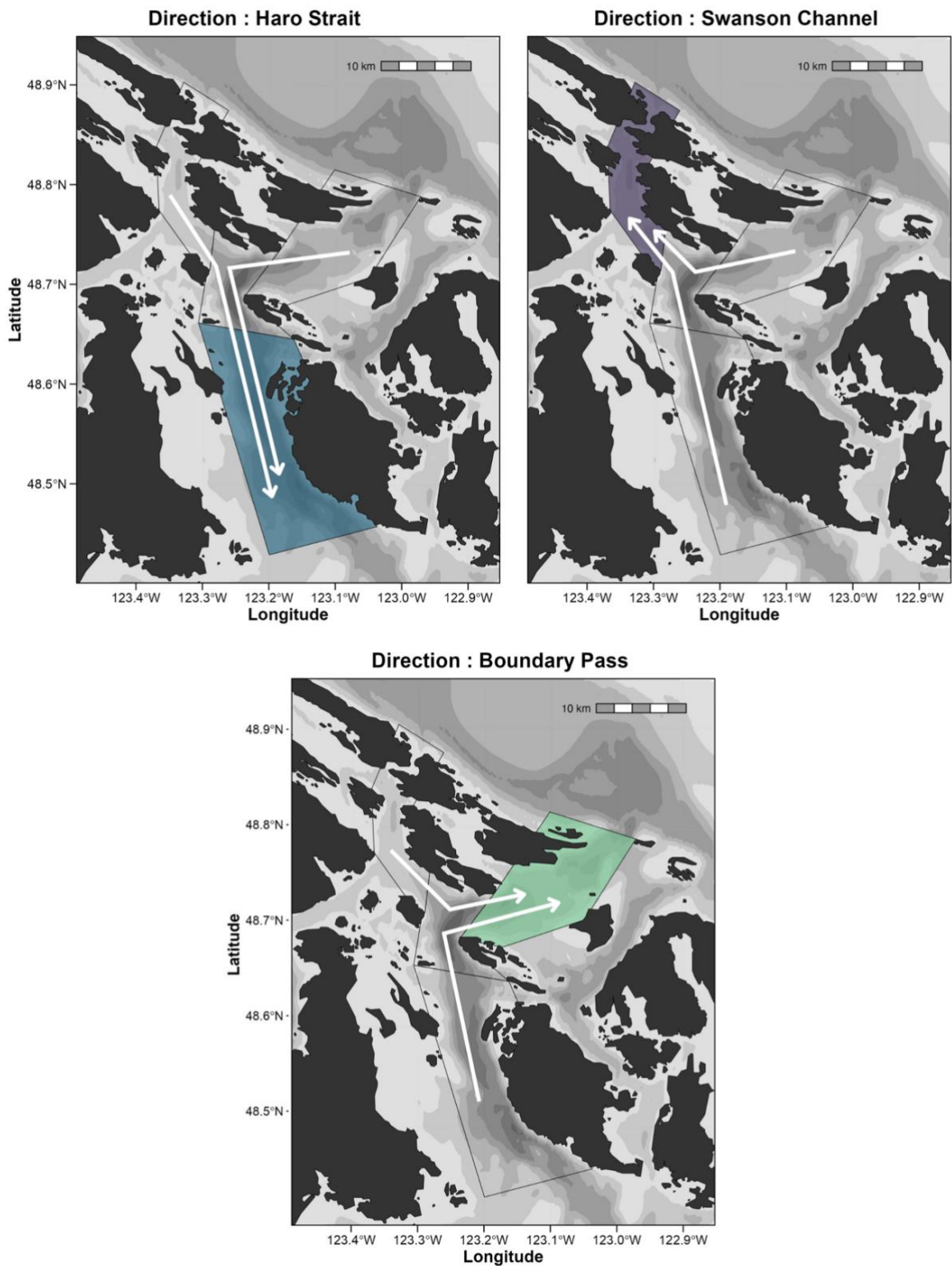


Figure 4. Schematic representation of the three categories of the multinomial models, illustrating behavioural trajectories (white arrows) crossing Rum Island and terminating in one of three directional zones: Haro Strait (blue), Swanson Channel (purple), or Boundary Pass (green). The background map shows the coastline, and bathymetry (grey scale).

Results

1. Descriptive analysis of Rum Island Soundscape

During the sampling period, meaning between September 9, 2023, and June 1, 2025, sampling period, broadband SPL (100–25,000 Hz), used to model SRKW movement trajectories, showed clear temporal variability (Fig. 5). High median and 95th percentile values of up to 110 dB were observed during the lunar months of spring and summer, while lower 95th percentile values of around 100 dB, were recorded during fall and winter. Notably, winter months showed elevated median SPL compared to other months, suggesting a persistently higher baseline. These results indicate a seasonal trend characterized by increased variability with more frequent high-amplitude acoustic events in summer and a noisier acoustic baseline in winter. Third-octave band analysis using Spearman's rank correlation confirmed significant associations with specific variables and supported the use of frequency-specific metrics to assess temporal trends in the soundscape.

1.1. Environmental variables and soundscape

Environmental variables mainly influenced the high-frequency components of the soundscape (Fig. 6). Wind speed showed the highest correlation with SPL at 8 kHz ($r_s = 0.350, p < 0.001$), while precipitation exhibited the strongest association at 20 kHz ($r_s = 0.346, p < 0.001$). Both variables showed positive correlations in mid-frequency bands starting around 500 Hz. In contrast, current speed had limited influence on the soundscape, showing only weak correlations at very high frequencies, observed primarily above 20 kHz ($r_s = 0.106, p < 0.001$). Wind and precipitation also showed weak positive correlations at lower frequencies.

Seasonal variations in environmental frequency-specific bands were evident (Fig. 7). Although precipitation is more frequent during winter, significantly higher median SPL in the 19.5–20.5 kHz band were observed in summer, with a median increase of 0.6 dB compared to winter ($p < 0.001$; Kruskal-Wallis test). Conversely, the wind-dominated 8 kHz band showed a more pronounced median 2 dB increase during winter ($p < 0.001$). Low-frequency SPL (10–100 Hz band) were significantly higher in winter ($p < 0.001$), but the summer 95th percentile low frequency SPL in this band rose by 7.93 dB, indicating more intense high-amplitude events.

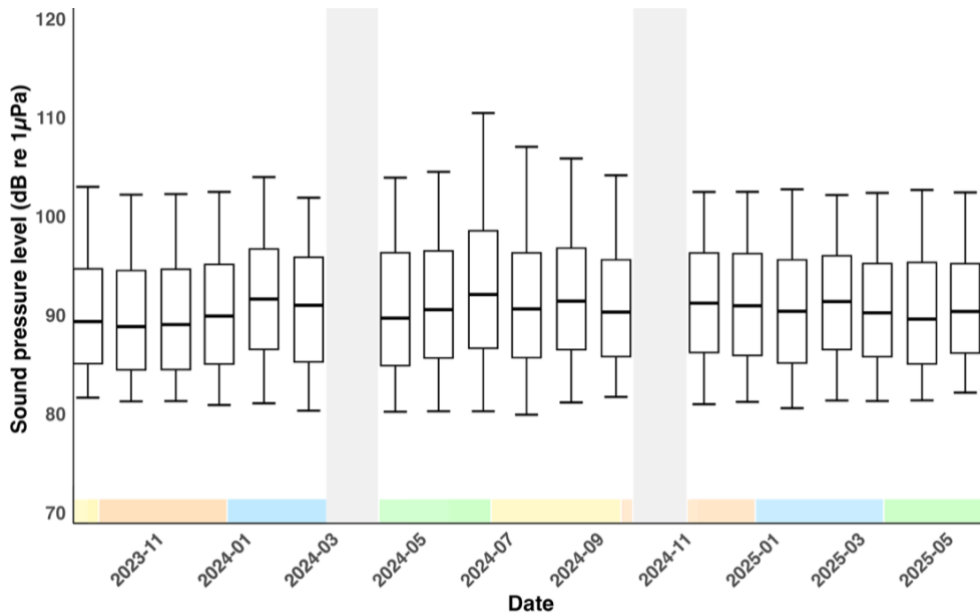


Figure 5. Box-and-whisker plots of 29-day lunar-month SPL in the 100-25000 Hz band. The plot displays median values (central line), interquartile range (box), and whiskers extended to the 5th and 95th percentiles. Bottom color represent the season with yellow: summer, orange: fall, blue: winter and green: spring. Grey area representing period of data loss.

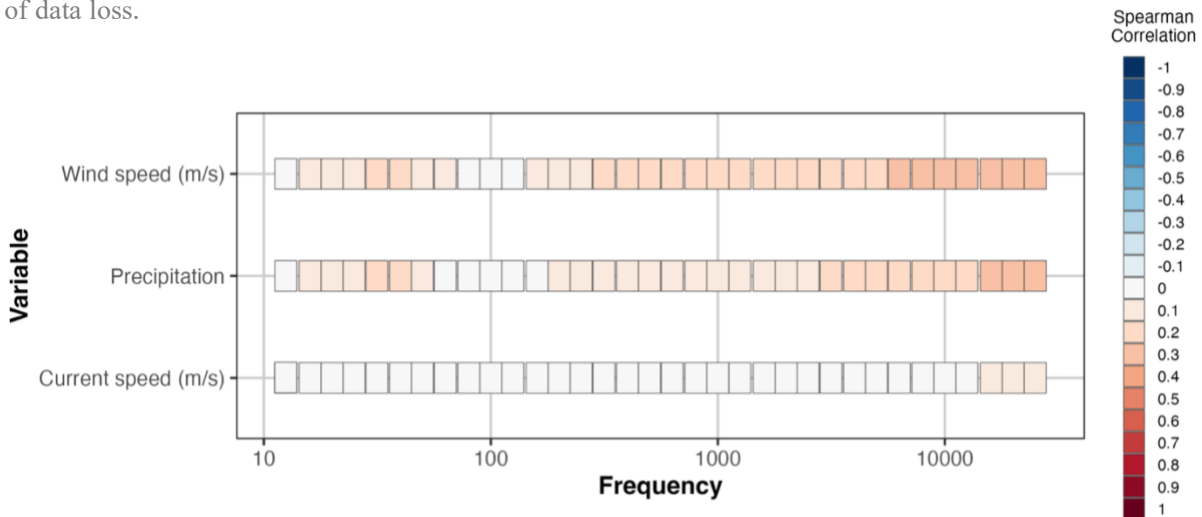


Figure 6. Heatmap of Spearman correlation coefficient for wind, precipitation and current for each 1/3 octave band SPL levels.

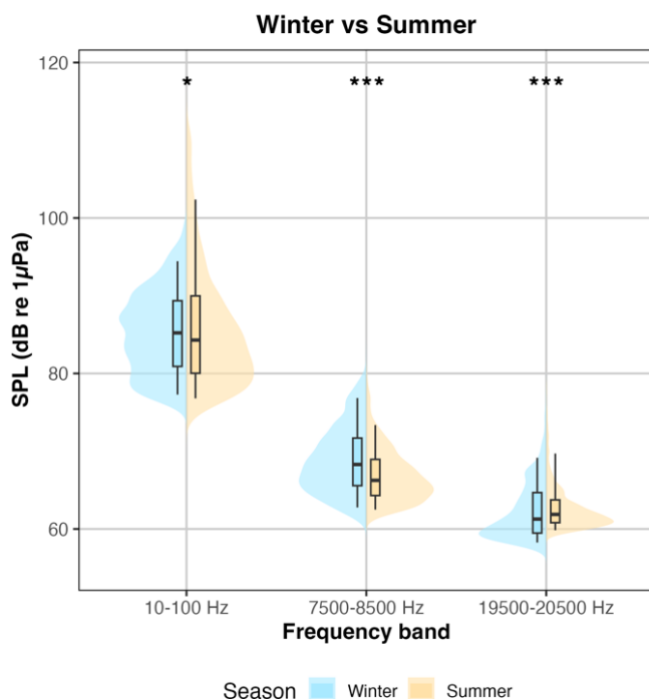


Figure 7. Box-and-whisker Summer-Winter comparison plots of SPL in the 10-100 Hz, 7500-8500 Hz, 19500-20500 Hz bands. The plot displays median values (central line), interquartile range (box), and whiskers extended to the 5th and 95th percentiles. (* = 0.05; ** = 0.01; *** = 0.001)

1.2. Shipping traffic and soundscape

The analysis of vessel traffic at Rum Island revealed stronger and broader acoustic impact on the Rum Island soundscape compared to environmental variables, with significantly higher correlation coefficients across frequency bands (Fig. 8). The cumulative noise metric, $L_{p, sum}$, representing all vessel categories (“All”), was associated with elevated correlation across a wide frequency range, showing prominent correlation peak between 100-1000 Hz, with a max at 315 Hz ($r_s = 0.618, p < 0.001$).

Cargo ships exhibited the strongest and most widespread influence, with significant positive correlations over a broad frequency spectrum and a peak in very low frequencies (<100 Hz), reaching a maximum at 80 Hz ($r_s=0.518, p < 0.001$). Tankers showed a similar pattern, with a correlation peak at 100 Hz ($r_s=0.211, p < 0.001$). Smaller vessel types, including small passenger boats, tugboats, sailing vessels, recreational boats, and fishing vessels, also showed frequency-wide correlations, but with a trend to affect higher frequency bands (above 100 Hz), and negative correlations in the low-frequency range (<100 Hz), except for tugboats which maintained a positive correlation throughout. Due to low number of recordings with large passenger vessel ($n=2,311$), there was insufficient power to find any significant correlations.

Vessel associated frequency bands exhibited clear seasonal patterns (Fig. 9). Median and L95 SPL in the 100-1000 Hz and 113-141 Hz bands were significantly higher during the summer months, with median increases of 1.9 dB and 2.5 dB respectively ($p < 0.001$), consistent with the greater volume of vessel transits observed during the summer season. In contrast, the 57-71 Hz band showed higher median SPL during winter, with a 2.3 dB increase ($p < 0.001$), however, the 10-100 Hz band had 2.8 dB higher L95 SPL in summer. This suggested the occurrence of more intense but less frequent acoustic events during the summer season in this low frequency band. Finally, the effectiveness of vessel slowdown measures was reflected in all three bands (Fig. 8), with box plots showing significantly lower SPL during slowdown periods. The largest reduction was observed in the 57-71 Hz band, with a median decrease of 3.7 dB ($p < 0.001$) and more modest noise reductions of 1.2 dB in the 100-1000 Hz band ($p < 0.001$) and L95 for all bands.

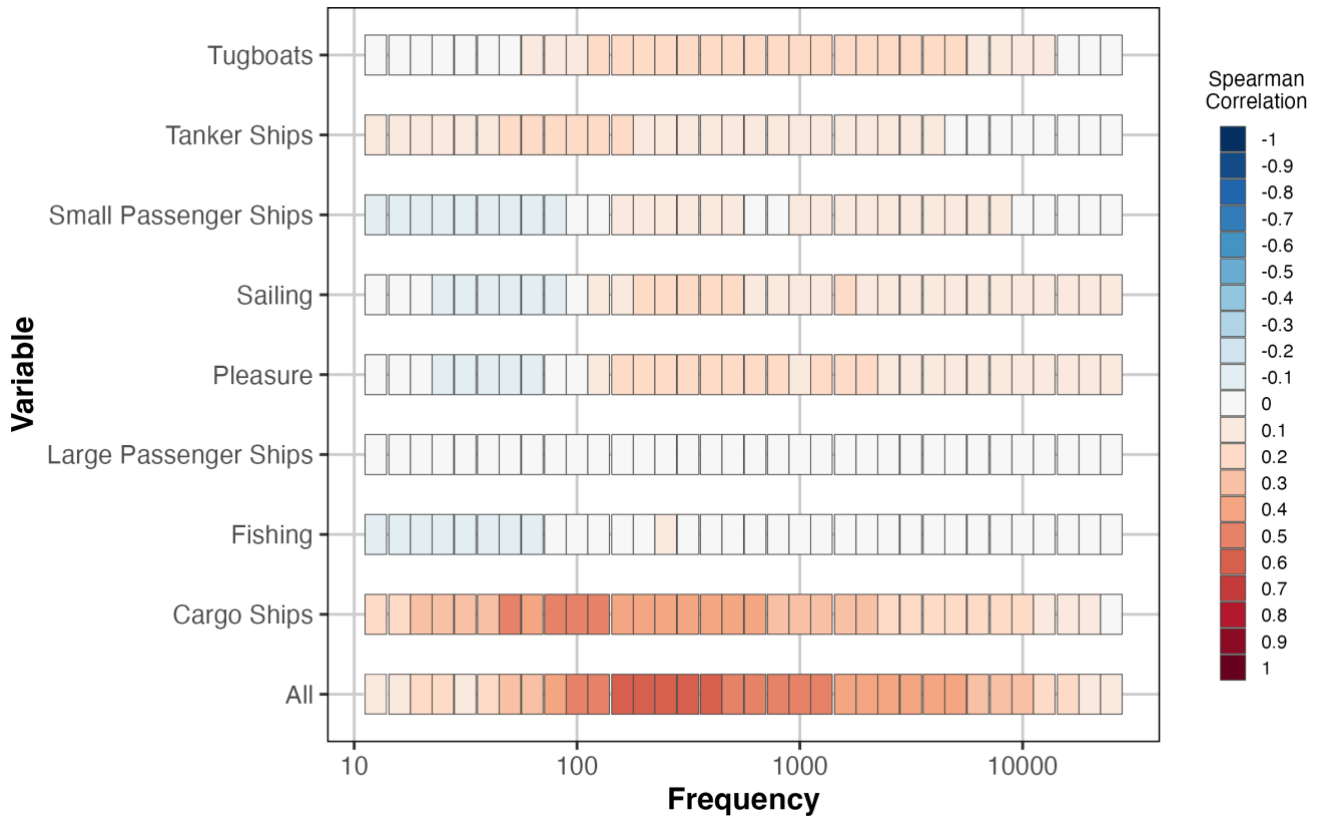


Figure 8. Heatmap of Spearman correlation coefficients between SPL values for each 1/3-octave band and the number of vessels (from AIS data) for different ship categories and for all ships combined ('All', bottom panel). The $L_{p,sum}$ metric was used to calculate vessel noise contribution for each correlation.

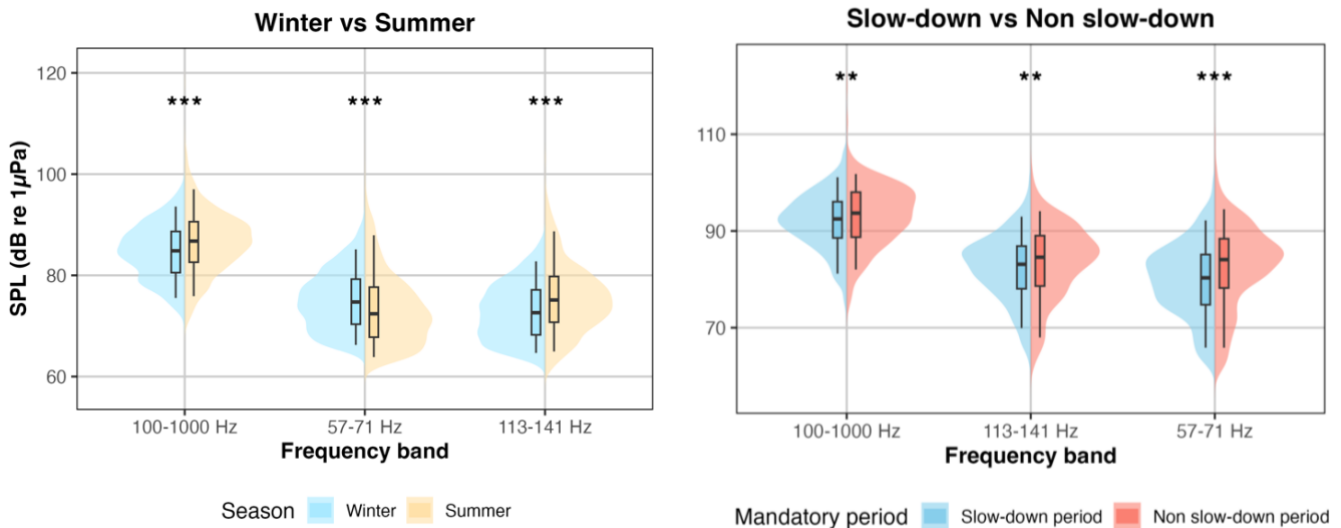


Figure 9. Box-and-whisker a) Summer-Winter b) mandatory comparison plots of SPL in the 100-1000 Hz, 57-71 Hz, 113-141 Hz bands. The plot displays median values (central line), interquartile range (box), and whiskers extended to the 5th and 95th percentiles. (* = 0.05; ** = 0.01; *** = 0.001)

2. Influence of soundscape and environment on SRKW trajectories

2.1. *Trajectory distribution*

A total of 628 SRKW visual and acoustic detections were recorded between September 9, 2023, and June 1, 2025, comprising 91% visual sightings and 9% acoustic detections. Most acoustic detections were made by the Rum Island hydrophone, with supplemental detections from Lime Kiln hydrophone (Haro Strait) and the East Point hydrophone (Boundary Pass). After applying filtering criteria and grouping detections into coherent movement sequences, we identified 69 trajectories transiting through Rum Island waters, representing 398 individual observations (Fig.10). Among these trajectories, 47.8% were oriented toward Swanson Channel (n=33), 40.6% towards Haro Strait (n=28), and only 11.6% toward Boundary Pass (n=8). This distribution indicates an uneven use of routes, with Boundary Pass being less frequented compared to the other channels. However, Boundary Pass is not an unfrequented area, as most observations in this channel were part of trajectories ultimately heading toward Haro Strait. The most observed movement patterns therefore consisted of trajectories originating in Haro Strait heading toward Swanson Channel, as well as those moving from Boundary Pass toward Haro Strait.

SRKW trajectories were more frequently observed during spring and summer months. Those heading toward Swanson Channel occurred consistently throughout the year (Fig.11) and represented a substantial portion of monthly movement, with a peak in July 2024 (n=4). Movements toward Haro Strait were predominantly spring/summer trajectories reaching a maximum in July (n=5). In contrast, the whales selected Boundary Pass direction sporadically across the year, with minor activity peaks in September 2023 (n=2) and October 2024 (n=2).

2.2. *Statistical model results*

Multicollinearity assessment of model predictors revealed moderate correlation between broadband SPL and ship count ($r_s = 0.489$, $p < 0.01$), therefore we retained only SPL as this predictor provided the best model fit (lowest AIC). This enabled clearer interpretation of the selected variable's effect and prevented inflated standard errors or unstable estimates due to collinearity. Model selection was performed using the AIC and the most parsimonious model (AIC = 63.3) included the following predictors:

$$\text{Direction} \sim s(\text{SPL Rum}) + s(\text{Current Speed}) + s(\text{Current Direction, bs = 'cc'}) \\ + s(\text{Month, bs = 'cc'}).$$

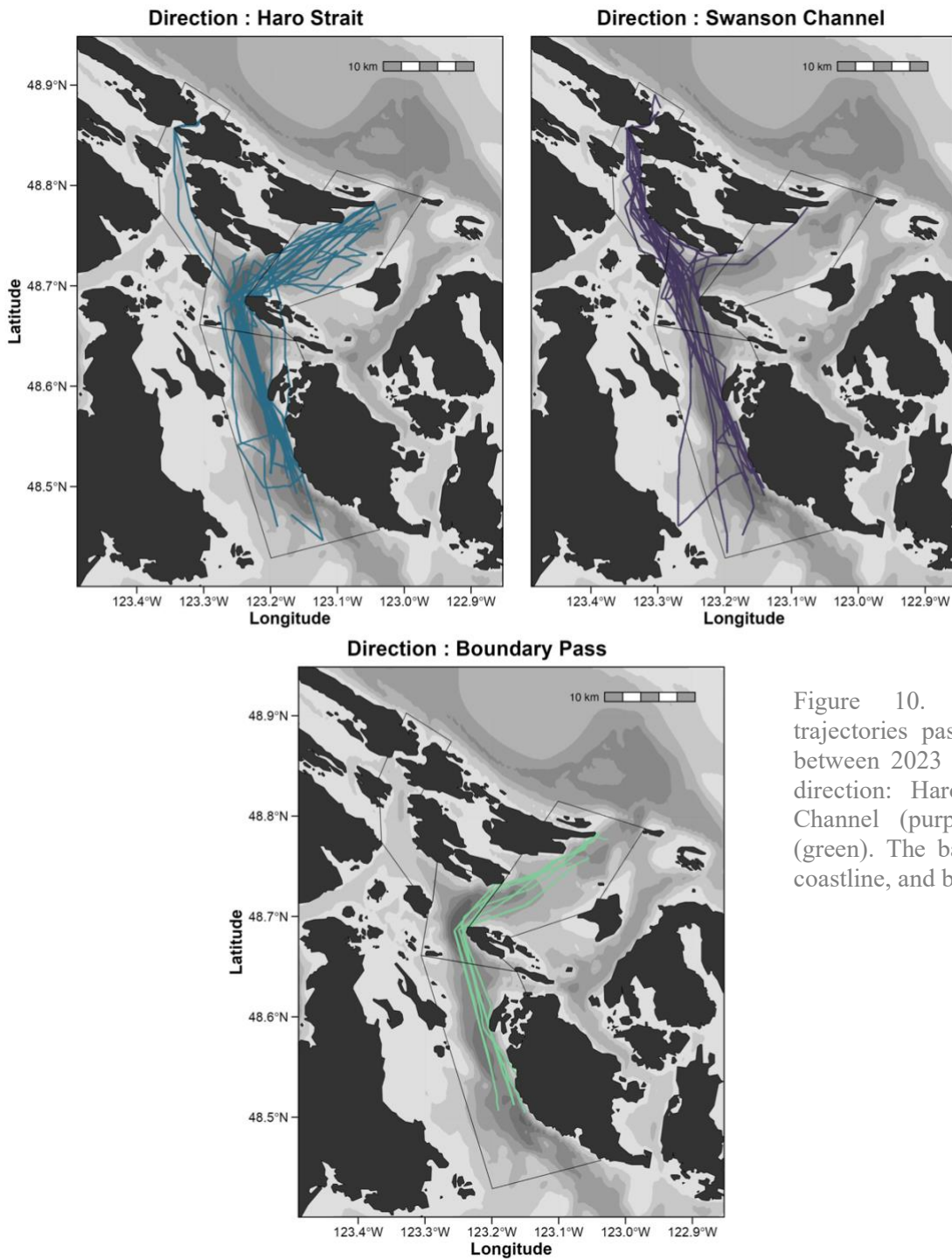


Figure 10. Map of reconstructed trajectories passing through Rum Island between 2023 and 2025, colored by exit direction: Haro Strait (blue), Swanson Channel (purple), and Boundary Pass (green). The background map shows the coastline, and bathymetry (grey scale).

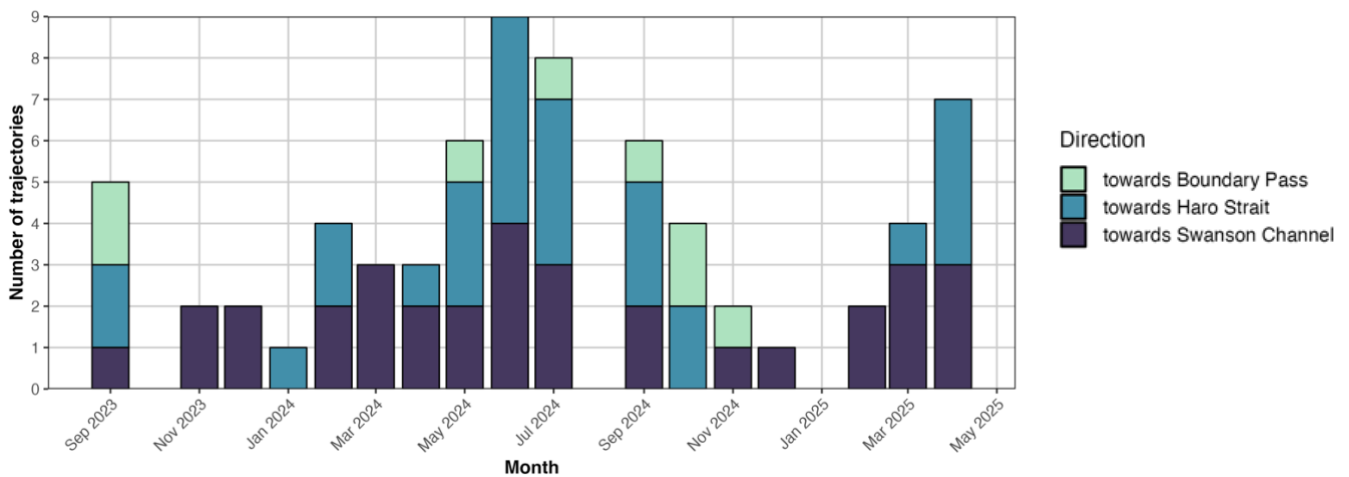


Fig 11. Histogram of temporal distribution for each trajectory types

Broadband SPL (100-25,000 Hz range) at Rum Island did not significantly influence route selection for either Haro Strait (EDF = 1, $\chi^2 = 0.004$, $p = 0.947$) or Swanson Channel (EDF = 1, $\chi^2 = 3.968$, $p = 0.057$) compared to Boundary Pass (Table 2). The partial effect plot for Haro Strait revealed a flat line, indicating no consistent variation in route probability across the observed SPL range (approximately 85 to 100 dB re 1 μ Pa). However, for Swanson Channel we found a (marginally) non-significant positive trend ($p = 0.056$), with route selection probability increased with higher SPL values (Fig. 12). For noise levels above 95 dB, the probability of selecting the route toward Swanson Channel exceeded that of the Boundary Pass reference route, peaking at a probability of 80% (Fig. 13). The probabilities for Haro Strait and Boundary Pass decreased under high SPL conditions, while Haro Strait showed a 50% selection probability under low SPL around 80 dB. This trend suggests a potential avoidance of Boundary Pass and Haro Strait or preference for Swanson Channel, under higher noise conditions. More trajectories would increase statistical power and strengthen confidence in the generalizability of our results.

Surface current speed significantly influenced route selection toward Haro Strait (EDF = 1.0, $\chi^2 = 5.06$, $p = 0.024$, Table.2). We found a linear increase in probability of selecting Haro Strait with increasing current speed, with a 100% route preference toward Haro Strait when current speeds reached >1.2 m/s (Fig. 13). In contrast, the effect of current speed on Swanson Channel was non-significant (EDF = 1.8, $\chi^2 = 5.27$, $p = 0.086$), with selection probability peaking at 60% for Swanson Channel at moderate current speeds ~ 0.5 m/s, before declining again to 53% for Boundary Pass in lower current speeds (~ 0.1 m/s) (Fig. 13). This may reflect occasional use of Swanson Channel under specific, favorable flow conditions, but the relationship appears less robust than for Haro Strait.

Surface current direction had a significant effect on route selection, with whales exhibiting a strong directional preference toward Haro Strait (EDF = 1, $\chi^2 = 5.060$, $p = 0.011$, Table.2). The partial effect of current direction showed a clear increase in selecting Haro Strait when current direction values ranged between 100° and 210° indicating south–southwest flow (Fig. 12) with the probability of selecting Haro Strait reached its maximum of 75% near 180° (Fig. 13). In contrast, current direction had no significant effect on the probability of selecting Swanson Channel ($p = 0.5037$). For this route, the partial effect was relatively flat with no dominant directional preference observable in predicted probabilities. Boundary Pass remained the least selected route across all current directions, with low and unstable selection probabilities.

Monthly patterns significantly influenced route selection for Swanson Channel (EDF = 1.95, $\chi^2 = 7.64$, $p = 0.0045$) but not for Haro Strait (EDF = 1.1, $p = 0.14$). The partial dependence plot for

	EDF	χ^2	p-val
<i>Toward Haro Strait</i>			
s(SPL_rum)	1.000	0.004	0.94692
s(Current Speed)	1.000	5.060	0.02449 *
s(Current Direction, bs=cc)	2.687	10.302	0.00573 **
s(Month, bs=cc)	1.105	1.821	0.14412
<i>Toward Swanson Channel</i>			
s(SPL_rum)	1.000	3.968	0.05636 .
s(Current Speed)	1.798	5.268	0.08615 .
s(Current Direction, bs=cc)	0.000	0.000	0.34455
s(Month, bs=cc)	1.952	7.642	0.00446 **

Table 2. Summary of smooth terms included in the multinomial GAM predicting SRKW route selection. Shown are the estimated degrees of freedom (EDF), chi-square statistics (χ^2), and p-values for each predictor, for both Haro Strait and Swanson Channel classes (relative to Boundary Pass). (. = 0.1; * = 0.05; ** = 0.01; *** = 0.001)

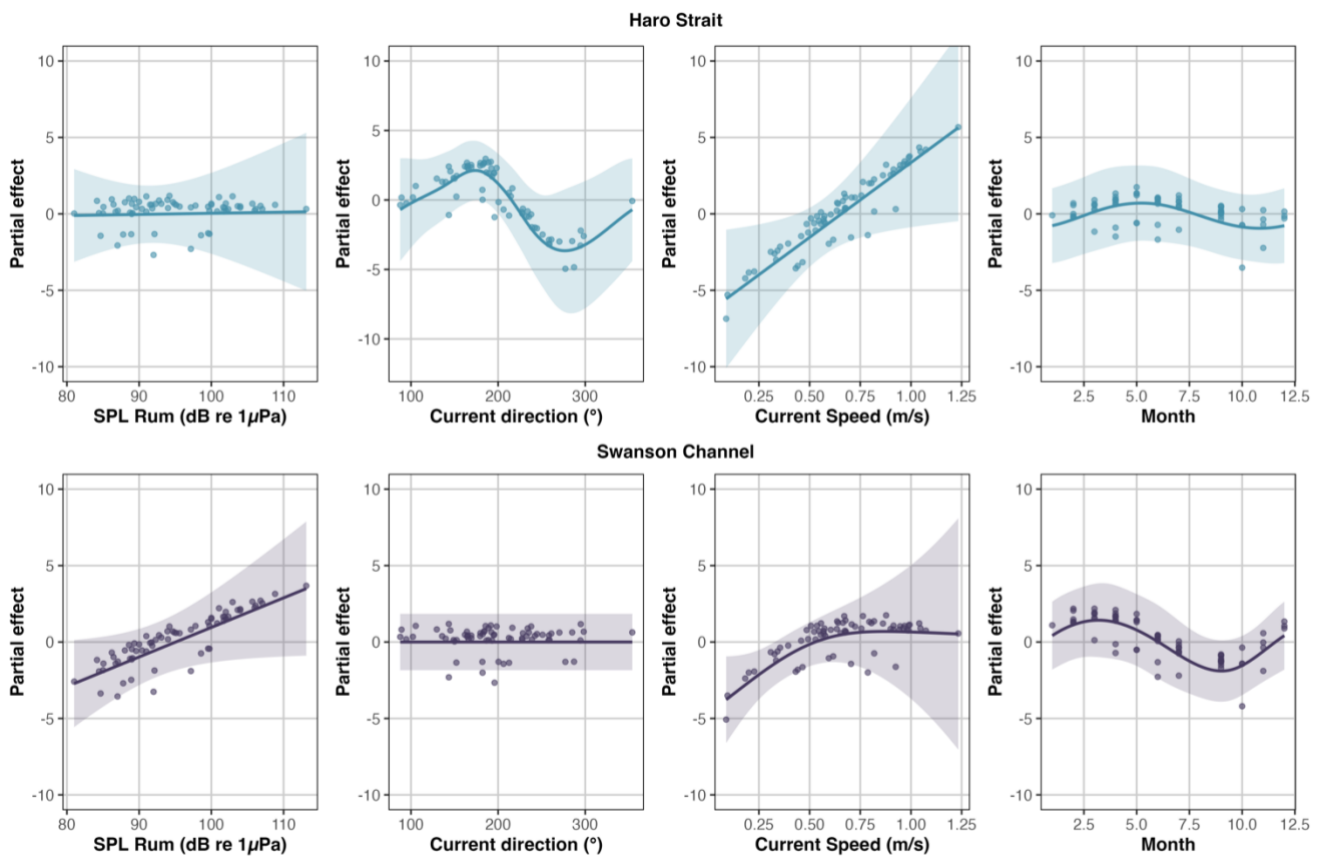


Figure 12. Partial Effect plots for each predictor include in the GAM model: Broadband SPL at Rum Island, surface current direction, surface current speed (cyclic) and month (cyclic). The y-axis represents the log-odds of selecting each route, Haro Strait (blue) and Swanson Channel (purple) relative to Boundary Pass.

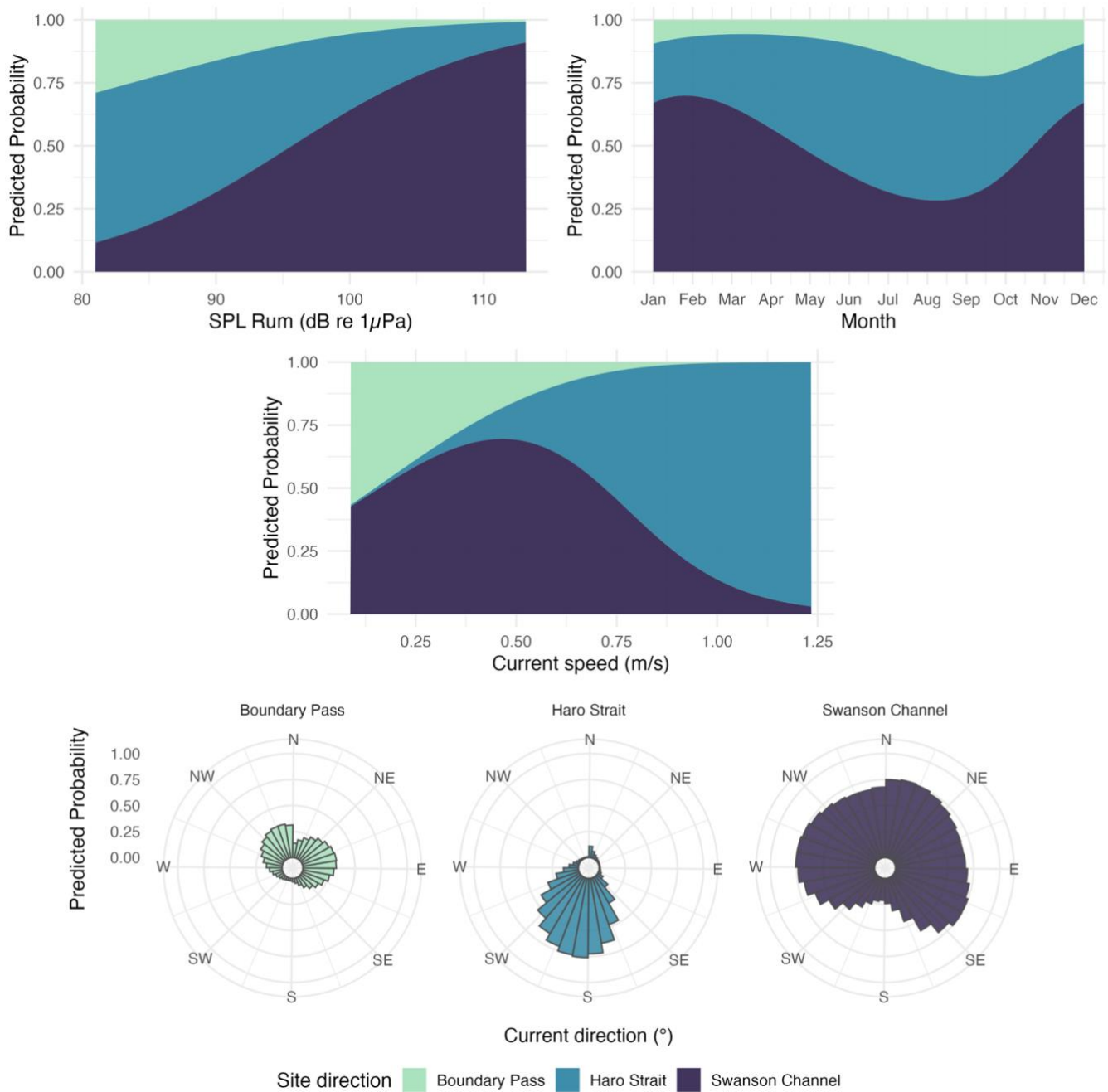


Figure 13. Predicted probabilities of SRKW route selection as a function of each explanatory variable, based on the fitted multinomial GAM. Probabilities are shown for each route option: Haro Strait (Blue), Swanson Channel (Purple), and Boundary Pass (Green), on a 0 to 1 scale.

Swanson Channel showed reduced selection probability during spring and summer months as compared to Boundary Pass (May to August) (Fig. 13), with a corresponding increase in the predicted probability of Haro Strait during this period. However, these results should be interpreted with caution and cannot be considered representative of true seasonal variation, as they are influenced by a bias in visual observations toward periods with higher sighting effort.

Discussion

This study examined the soundscape of Rum Island and investigated how SRKW responded to variability in their environment by assessing the combined influence of soundscape noise and hydrodynamics conditions on their movement decisions. We revealed how the acoustic environment at Rum Island is structured, and how broadband SPL and hydrodynamic variability influenced SRKW route selection. These results partly supported our hypothesis that the soundscape at Rum Island was primarily driven by maritime traffic, and that SRKW movements through different corridors were shaped by a combination of acoustic disturbance and hydrodynamics conditions.

Among the 69 reconstructed trajectories that passed by Rum Island, two dominant routing patterns emerged: (1) the route from Haro Strait to Swanson Channel, and (2) the route from Boundary Pass to Haro Strait. In contrast, trajectories heading toward Boundary Pass from Rum Island were much less frequent, suggesting a lower likelihood of selection for this corridor during route selection at Rum Island. This could be driven by local environmental or anthropogenic factors. While these patterns have been anecdotally observed in the past, they have never been documented in the literature. Although no pod-level analysis was conducted, these observed patterns correspond well with the spatial distribution of SRKW pods described by Hauser et al. (2007), with J pod more frequently observed yearly in Swanson Channel, K pod more often in Boundary Pass, and L pod occupying an intermediate range, though all pods are regularly present in Haro Strait.

1. Soundscape at Rum Island: a noisy crossroad?

To better understand if acoustic disturbance influenced movement corridor preferences at Rum Island, we evaluated how measured broadband SPL was reflected by ship presence and disturbance in SRKW habitat. Median broadband SPL measured at Rum Island were relatively low compared to adjacent areas such as Boundary Pass or Haro Strait, where Burnham et al. (2021) reported median values between 115–125 dB. This difference may be partly explained by methodological factors such as hydrophone sensitivity and deployment depth, which may underestimate received levels, particularly at higher frequencies, given that the variability observed across the different bands is similar.

Environmental variables, mainly wind and precipitation, influence the mid and high-frequency components of the soundscape, particularly during the winter months. Consistent with previous findings from the Salish Sea (Burnham et al. 2021), wind exhibited correlation peaks around 8 kHz, while precipitation primarily affects frequency bands centered near 20 kHz with a moderate effect observed in the low frequency, where median sound levels were higher in winter than in summer. This winter increase may have resulted from a combined effect of meteorological conditions and acoustic propagation. During winter in the Salish Sea, Eickmeier et al. (2021) reported a surface thermocline that created an acoustic channel that traps sound near the surface, reducing transmission loss and favouring higher ambient SPL. However, unlike other frequency bands, the high-frequency precipitation band showed higher SPL during summer. This pattern, despite the generally stronger and more frequent rainfall events in winter, may be explained by the overlap with other high-frequency noise sources in summer, particularly due to the intensification of recreational vessel traffic. Although several other studies (e.g., Basan et al. 2024) have reported increased current speeds correlate with elevated low-frequency sound levels, this effect was not observed in our study, likely due to the shallow, coastal deployment of the Rum Island hydrophone which limits the listening range for detecting this soundscape component, compared to more exposed offshore regions.

Ship traffic constituted the main source of acoustic disturbance at Rum Island, affecting the frequency spectrum below 24 kHz, with peak intensity below 1 kHz. This was particularly pronounced during summer and daytime periods. Cargo ships and tankers generated high-amplitude, low-frequencies noise (<100 Hz). Their passages past Rum Island resulted in distinct acoustic events, visible in the high percentiles (L95) of the specific bands, even in winter. In contrast, smaller vessels produced noise in mid to high frequencies above 500 Hz. Since the region is a population boating destination for both Canadian and American boaters, small recreational boats are likely contributing to the elevated levels observed in summer in the >500 Hz and in bands up to 20 kHz. The summer intensification of traffic across all vessel types, led to both elevated background noise and irregular acoustic peaks not seen in the winter soundscape analysis (Veirs & Veirs, 2005). In winter, the soundscape is dominated by commercial vessels which maintained a constant presence. This could explain the persistently high 95th percentile levels in the low-frequency specific bands during this season. Finally, regional ship speed reduction measures enacted between June and November appeared to have a beneficial effect, with 2 dB reduction in SPL in the relevant frequency bands. This reduction has been recognized as significant in some studies for SRKW, improving foraging efficiency (Joy et al. 2019).

Class B vessels, such as whale-watching boats, recreational crafts, and small fishing vessels, are underrepresented or absent in the AccessAIS data since these vessel types were not required to have an AIS transponder. Considering the high density of non-AIS vessels, especially recreational boats in the Salish Sea engaged in wildlife viewing of SRKW during summer, with up to 50 boats observed surrounding a single pod, it was assumed that the acoustic contribution would be substantial despite being poorly quantified. As these vessel types carry depth sounders that rely on a high-frequency active acoustic signal, some studies have suggested that monitoring frequency bands around 50 kHz can improve detection of these smaller vessels due to the depth-sounder sonars that emit in this specific frequency range (Burnham et al. 2021).

We observed a frequency overlap between environmental variables in the low-frequency range (<100 Hz) as well as around the ~500 Hz bands. However, as demonstrated by Burnham et al. 2021 and confirmed by the disparity in our correlation analysis analyzing environmental variables and anthropogenic variables, ship noise consistently dominates the soundscape through intense, intermittent events. These ship events impacted frequency bands related to SRKW communication (500–15,000 Hz) and echolocation (15–100 kHz) (Burnham et al. 2023), even when ambient noise components are also present at comparable intensities (Heise et al. 2017). Taken together, it is likely that anthropogenic impacts on ambient soundscape observed at Rum Island is contributing to behavioural responses including SRKW routing decisions.

2. Routes adjustments to environmental conditions

The multinomial model results did not reveal a significant effect of broadband SPL on the routing decisions of SRKW, however, a clear trend emerged: Probability to select Swanson Channel increased with higher SPL broadband values. Although not statistically significant, this pattern must be interpreted with caution and considered an exploratory indication rather than confirmed evidence of SRKW avoiding noisier routes in favor of a relatively quieter path through Swanson Channel. This trend is consistent with previous studies documenting SRKW behavioural responses to acoustic disturbances, such as increased dive durations, higher swim speeds, abrupt trajectory shifts, and long-term spatial avoidance of key foraging grounds or socialization areas (Williams et al. 2006). Reported behavioural response thresholds vary among studies but generally range around 120 dB re 1 μ Pa for broadband SPL (Erbe, 2002), with responses sometimes observed as low as 109–116 dB (Williams et al. 2002). The broadband SPL response recorded in this study mostly fell below those thresholds (i.e., Rum Island was 95 dB re 1 μ Pa), although soundscape levels may be underestimated compared to other sites due to different measurement conditions or different exposure context.

This potential response to the soundscape is more likely linked to anthropogenic noise than to natural environmental noise. In fact, as observed in soundscape analysis at Rum Island, vessel noise spanned wide frequency bands, including those used by SRKW for communication (500–15,000 Hz) and echolocation (>15,000 Hz), with persistent episodic SPL peaks. The SPL broadband levels associated with increased likelihood of SRKW selecting Swanson Channel (95–110 dB) typically corresponded to high percentiles (75th, 95th, (Fig.5)), suggesting a negative behavioural response to Boundary Pass or Haro Strait trajectories in intense but infrequent noise events recorded from maritime traffic. This hypothesis is supported by the high correlation between broadband SPL and ship density in the multinomial GAM full model. In contrast, environmental noise factors such as wind and precipitation were stronger in winter but were generally more constant (not episodic) in the region. In other studies, these environmental noise factors are habitat cues and not considered disturbance, however species such as humpback whales have exhibited a reduced behavioural response to some environmental noise, compared to ship-derived noise (Fournet et al. 2018).

Swanson Channel noise levels were quieter than those of adjacent Boundary Pass and Haro Strait, and as such may provide an acoustic refuge to SRKW. Alternatively, the potential preference for Swanson Channel may reflect an avoidance of the noisier regions of Haro Strait and Boundary Pass. Both these channels were heavily trafficked by international commercial vessels (as shown by $L_{p, sum}$ maps (Fig.2)). Nonetheless, the northern region of Swanson Channel is frequented by large ferries operating between Vancouver's Tsawwassen Ferry Terminal and Vancouver Island's Schwartz Bay Ferry Terminal, whose acoustic footprint should not be overlooked, even if less intense than commercial shipping elsewhere. It is also plausible that the observed routing toward Swanson Channel under elevated acoustic conditions may reflect a pre-determined movement plan, with high SPL in Rum Island increasing the navigation speed toward that corridor rather than redirecting movement. However, no studies have specifically addressed this navigation route, and no acoustic data from Swanson Channel are available to confirm its potential role as a quieter alternative or even a high foraging ground for this population.

The correlation observed between trajectories toward Haro Strait and fast surface currents flowing south-southwest suggests that SRKWs take advantage of tidal and estuarine water movements to optimize energy expenditure during their movements (Fig.14). This pattern reflects the influence of the unique hydrodynamic setting of the Salish Sea, a semi-enclosed estuarine system governed by a mixed semi-diurnal tidal regime. Tidal flows oscillate northward during flood tides, driven by Pacific Ocean inflow through the Strait of Juan de Fuca, and southward during ebb tides. These are punctuated by slack water periods during high and low tide (Yang et al. 2020).

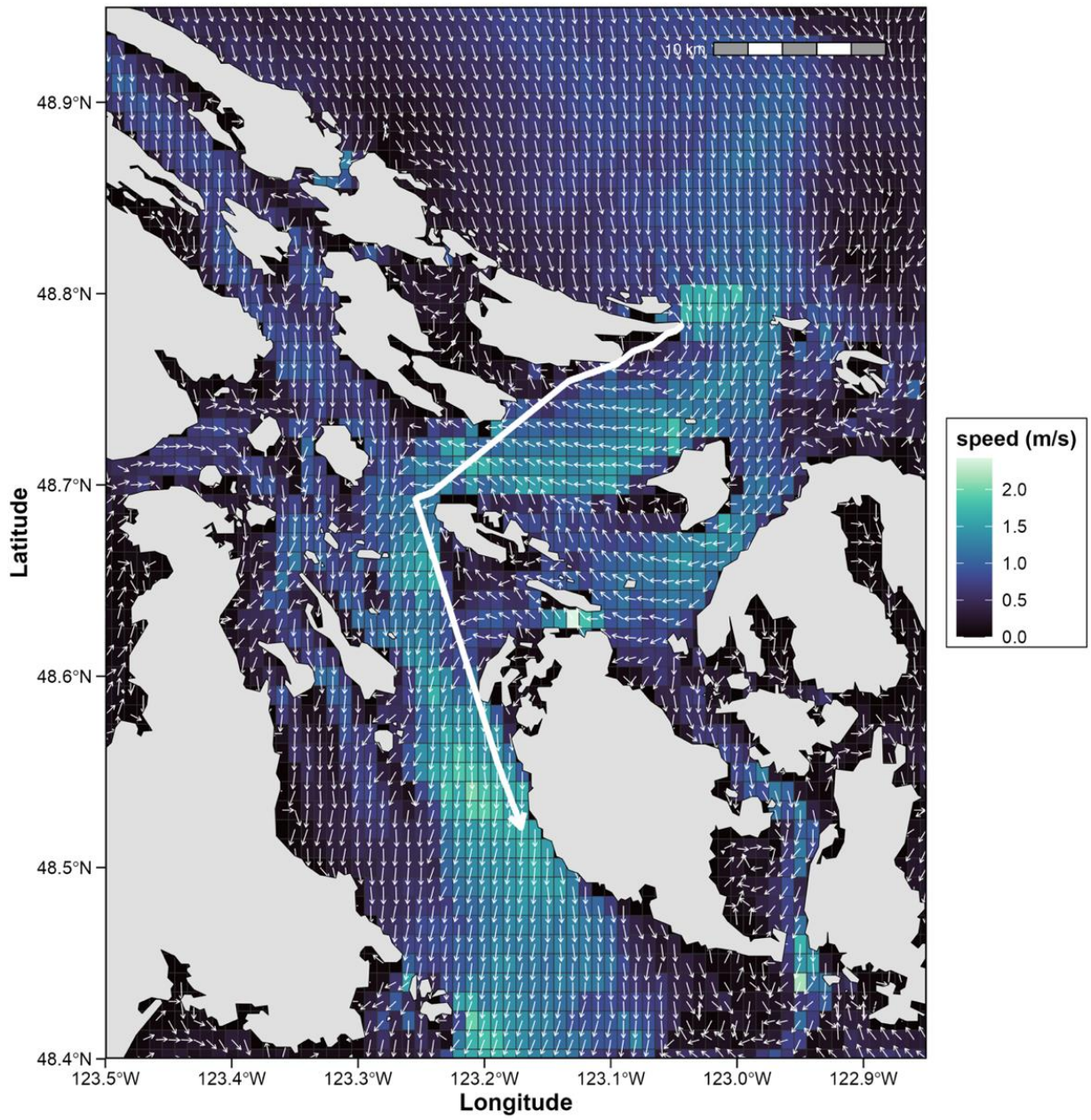


Figure 14. Current speed (color scale) and direction (white arrow) for one trajectory going towards Haro Strait from Boundary Pass happened May 29, 2024.

Superimposed on this tidal oscillation is a net estuarine flow, primarily driven by freshwater discharge from the Fraser River (Stang et al. 2025). This flow strengthens in spring and summer, enhancing the persistent southward surface current (0–50 m depth) through Boundary Pass and Haro Strait. SRKWs may exploit both ebb tides and net estuarine outflow to reduce energetic costs when traveling from Boundary Pass to Haro Strait. This strategy aligns with earlier findings of current-assisted movement in this population, particularly when current speeds exceed 1 m/s (Soucy, 2006).

Moreover, SRKW primarily forage on Chinook salmon in the Salish Sea, whose migrations are also modulated by tidal patterns by moving upstream during flood tides and slow down during ebb tides to resist the outward tidal flow (Stasko et al. 1973). By aligning with the ebb tide, SRKWs may gain faster access to foraging hotspots like Lime Kiln in Haro Strait, known for high Chinook densities and easiest prey to catch due to current. This is consistent with a summer increase in use of Haro Strait observed in our data.

Overall, routing decisions at the strategic junction of Rum Island appear to result from a multi-criteria trade-off involving anthropogenic exposure, hydrodynamics conditions, and foraging opportunity. The observed route adjustments reflect a trade-off between anthropogenic risk and energetic efficiency. Avoiding noisier corridors may require longer transits, exposure to less favourable currents, and passage through areas with lower foraging opportunities. Repeated avoidance of critical yet acoustically degraded corridors like Boundary Pass could lead to functional fragmentation of key high-density foraging areas. For SRKWs, whose survival is already constrained by declining Chinook abundance, any increase in travel costs may further narrow their limited energetic margin needed to maintain short-term needs such as maintaining body condition, reproduction, or care for calves. Over time, this reduced energy intake may compromise individual fitness and further threaten the long-term viability of this endangered population.

Beyond these ecological adaptations, movement trajectories may also be shaped by culturally transmitted behaviours. The social structure of SRKW supports vertical transmission of behavioural strategies, allowing knowledge and traditions to persist across generations (Auguin et al. 2025). In this context, routing decisions observed at Rum Island may reflect socially transmitted, long-term learned responses to environmental and anthropogenic conditions. Furthermore, the differential use of movement corridors might be influenced by the social composition of the groups transiting through Rum Island. Ford et al. (2000) demonstrated that certain pod combinations tend to be spatially driven by one dominant pod, suggesting that internal social structure can guide group-level movements. This social component may have introduced pseudo-replication, which can artificially narrow confidence

intervals and produce smaller p-values, potentially overestimating the statistical significance of variable effects.

The absence of significant soundscape effects should not be interpreted as evidence of no influence, but rather a reflection of the behavioural complexity of these intelligent and social animals, exacerbated by the methodological and contextual limitations such as the low number of reconstructed trajectories, uneven seasonal sampling, and the use of broadband SPL. Using broadband SPL as the acoustic variable provided a general estimate but did not isolate specific noise sources or accurately account for received levels at the whale's location. Refining analyses through biologically weighted Sound Exposure Levels (SELs) based on the audiogram of the SRKW would allow for a more precise assessment of acoustic risk by incorporating several key factors (Erbe, 2011). These include the relationship between the sound source and the SRKW, such as the position of commercial vessels relative to the whales, environmental variables that affect sound propagation, and the SRKWs hearing sensitivity, particularly within the 500 Hz to 15 kHz frequency range which is directly impacted by vessel noise but diluted in our broadband SPL measurements (Branstetter et al. 2017; Tougaard et al. 2019). Furthermore, as highlighted by Ellison et al. (2011), behavioural responses depend heavily on the context of exposure, including the behavioural state at the time of exposure, signal novelty, signal-to-noise ratio, and exposure history, factors that are difficult to incorporate into models, thus contributing to uncertainty.

While this study supports the hypothesis that SRKW trajectories are shaped by both anthropogenic and hydrodynamic factors, longer-term monitoring is needed to fully capture these patterns. A priority should be a comprehensive acoustic impact assessment across all movement corridors, with particular focus on Swanson Channel, which may act as an acoustic refuge, with a broader perspective on other key routes such as Rosario Strait, an important corridor especially for the J-pod (Olson et al. 2018). Future work should integrate developed acoustic metrics (e.g. SELs), hydrodynamics conditions, and trophic contexts at the pod level to better understand the ecological trade-offs involved in accessing physically and trophically favourable areas. From a conservation perspective, our results support the strategic implementation of vessel slowdown measures in critical areas like Rum Island, where they could help reduce acoustic barriers to important movement corridors. Targeted management actions such as enhanced noise mitigation and maritime traffic regulation, could additionally strengthen the resilience of this endangered population and minimize disturbance across the corridors essential to its survival.

Conclusion

In conclusion, this study highlights the predominant impact of maritime traffic on the soundscape of Rum Island, as well as the combined influence of this acoustic environment and hydrodynamics conditions on the routing decisions of Southern Resident Killer Whales across the three main navigation corridors. It provides new insights into the acoustic and spatial dynamics of SRKWs in the Southern Gulf Islands, underscoring the strategic role of Rum Island as a central decision point and the potential importance of Swanson Channel as an acoustic refuge. The results confirm the significance of Haro Strait for this population, particularly when currents are favourable, and support the effectiveness of vessel slowdown measures in reducing acoustic disturbance created by marine traffic, which may in turn influence SRKW habitat use and movement corridors. These findings reinforce the need to focus management and conservation efforts in key movement corridors to limit anthropogenic pressures while maintaining access to essential habitats. In the long term, integrating finer-scale data on acoustic exposure, trophic dynamics, and culturally transmitted movement traditions will allow a better understanding of the ecological trade-offs that shape the mobility of this endangered population.

Bibliography

- (1) Auguin, E., Guinet, C., Mourier, J., Clua, E. E. G., Gasco, N., & Tixier, P. (2025). The role of social transmission in the use of a new behaviour by killer whales in response to fisheries. *Animal Behaviour*, 225, 123228. <https://doi.org/10.1016/j.anbehav.2025.123228>
- (2) Basan, F., Fischer, J.-G., Putland, R., Brinkkemper, J., De Jong, C. A. F., Binnerts, B., Norro, A., Kühnel, D., Ødegaard, L.-A., Andersson, M., Lalander, E., Tougaard, J., Griffiths, E. T., Kosecka, M., Edwards, E., Merchant, N. D., De Jong, K., Robinson, S., Wang, L., & Kinneking, N. (2024). The underwater soundscape of the North Sea. *Marine Pollution Bulletin*, 198, 115891. <https://doi.org/10.1016/j.marpolbul.2023.115891>
- (3) Branstetter, B. K., St. Leger, J., Acton, D., Stewart, J., Houser, D., Finneran, J. J., & Jenkins, K. (2017). Killer whale (*Orcinus orca*) behavioural audiograms. *The Journal of the Acoustical Society of America*, 141(4), 2387–2398. <https://doi.org/10.1121/1.4979116>
- (4) Burnham, R. E., Vagle, S., & O'Neill, C. (2021). Spatiotemporal patterns in the natural and anthropogenic additions to the soundscape in parts of the Salish Sea, British Columbia, 2018–2020. *Marine Pollution Bulletin*, 170, 112647. <https://doi.org/10.1016/j.marpolbul.2021.112647>
- (5) Burnham, R., Vagle, S., Thupaki, P., & Thornton, S. (2023). Implications of wind and vessel noise on the sound fields experienced by southern resident killer whales *Orcinus orca* in the Salish Sea. *Endangered Species Research*, 50, 31–46. <https://doi.org/10.3354/esr01217>
- (6) ELLISON, W. T., SOUTHALL, B. L., CLARK, C. W., & FRANKEL, A. S. (2012). A New Context-Based Approach to Assess Marine Mammal Behavioural Responses to Anthropogenic Sounds. *Conservation Biology*, 26(1), 21–28. <https://doi.org/10.1111/j.1523-1739.2011.01803.x>
- (7) Erbe, C. (2011). *A Pocket Handbook 3rd Edition*.
- (8) Erbe, C. (2002). UNDERWATER NOISE OF WHALE-WATCHING BOATS AND POTENTIAL EFFECTS ON KILLER WHALES (*ORCINUS ORCA*), BASED ON AN ACOUSTIC IMPACT MODEL. *Marine Mammal Science*, 18(2), 394–418. <https://doi.org/10.1111/j.1748-7692.2002.tb01045.x>
- (9) Erbe, C., Dunlop, R., & Dolman, S. (2018). Effects of Noise on Marine Mammals. In H. Slabbekoorn, R. J. Dooling, A. N. Popper, & R. R. Fay (Eds.), *Effects of Anthropogenic Noise on Animals* (Vol. 66, pp. 277–309). Springer New York. https://doi.org/10.1007/978-1-4939-8574-6_10
- (10) Fisheries and Oceans Canada. "2025 Management Measures to Protect Southern Resident Killer Whales." Government of Canada. Last modified July 15, 2025. Accessed August 4, 2025. <https://www.pac.dfo-mpo.gc.ca/fm-gp/mammals-mammiferes/whales-baleines/srkw-measures-mesures-ers-eng.html>.

- (11) Ford, J. K. B., Pilkington, J. F., Reira, A., Otsuki, M., Gisborne, B., Abernethy, R. M., Stredulinsky, E. H., Towers, J. R., & Ellis, G. M. (2017). *Habitats of Special Importance to Resident Killer Whales (*Orcinus orca*) off the West Coast of Canada*.
- (12) Ford JKB, Ellis GM, Balcomb KC (2000) *Killer whales*, UBC Press, Vancouver
- (13) Fournet, M., Matthews, L., Gabriele, C., Haver, S., Mellinger, D., & Klinck, H. (2018). Humpback whales *Megaptera novaeangliae* alter calling behaviour in response to natural sounds and vessel noise. *Marine Ecology Progress Series*, 607, 251–268. <https://doi.org/10.3354/meps12784>
- (14) Frisk, G. V. (2012). Noiseconomics: The relationship between ambient noise levels in the sea and global economic trends. *Scientific Reports*, 2(1), 437. <https://doi.org/10.1038/srep00437>
- (15) Gibson, R. Go with the flow: tidal migration in marine animals. (2003). *Hydrobiologia* 503, 153–161 <https://doi.org/10.1023/B:HYDR.0000008488.33614.62>
- (16) Hauser, D., Logsdon, M., Holmes, E., VanBlaricom, G., & Osborne, R. (2007). Summer distribution patterns of southern resident killer whales *Orcinus orca*: Core areas and spatial segregation of social groups. *Marine Ecology Progress Series*, 351, 301–310. <https://doi.org/10.3354/meps07117>
- (17) Heise, K., Barrett-Lennard, L., Chapman, R., Dakin, T., Erbe, C., Hannay, D., Merchant, N., Pilkington, J., Thornton, S., Tollit, D., Vagle, S., Veirs, V., Vergara, V., Wood, J., Wright, B., & Yurk, H. (2017). *PROPOSED METRICS FOR THE MANAGEMENT OF UNDERWATER NOISE FOR SOUTHERN RESIDENT KILLER WHALES*. <https://doi.org/10.25317/CORI20172>
- (18) Holt, M. (2008). *NOAA Technical Memorandum NMFS-NWFSC-89. Sound Exposure and Southern Resident Killer Whales (*Orcinus orca*): A Review of Current Knowledge and Data Gaps*.
- (19) Joy, R., Tollit, D., Wood, J., MacGillivray, A., Li, Z., Trounce, K., & Robinson, O. (2019). Potential Benefits of Vessel Slowdowns on Endangered Southern Resident Killer Whales. *Frontiers in Marine Science*, 6, 344. <https://doi.org/10.3389/fmars.2019.00344>
- (20) JASCO Applied Sciences. (2014). Underwater acoustic modeling report for the Roberts Bank Terminal 2 Technical Report. Vancouver Fraser Port Authority.
- (21) Lin, T.-W., Dowd, M., & Joy, R. (2025). Forecasting trajectories of Southern Resident killer whales with stochastic movement models incorporating direction modification. *Ecological Modelling*, 509, 111254. <https://doi.org/10.1016/j.ecolmodel.2025.111254>
- (22) Murray, C. C., Hannah, L. C., Doniol-Valcroze, T., Wright, B. M., Stredulinsky, E. H., Nelson, J. C., Locke, A., & Lacy, R. C. (2021). A cumulative effects model for population trajectories of resident killer whales in the Northeast Pacific. *Biological Conservation*, 257, 109124. <https://doi.org/10.1016/j.biocon.2021.109124>

- (23) Olson, J., Wood, J., Osborne, R., Barrett-Lennard, L., & Larson, S. (2018). Sightings of southern resident killer whales in the Salish Sea 1976-2014: The importance of a long-term opportunistic dataset. *Endangered Species Research*, 37, 105–118. <https://doi.org/10.3354/esr00918>
- (24) Soontiens, N., & Allen, S. E. (2017). Modelling sensitivities to mixing and advection in a sill-basin estuarine system. *Ocean Modelling*, 112, 17–32. <https://doi.org/10.1016/j.ocemod.2017.02.008>
- (25) Soucy, E. M. (2006). *Patterns of Southern Resident killer whale (Orcinus orca) Movement in Relation to Tides and Currents*.
- (26) Stang, C., & Allen, S. E. (2025). Seasonably Variable Estuarine Exchange Through Interconnected Channels in the Salish Sea. *Journal of Geophysical Research: Oceans*, 130(5), e2024JC022003. <https://doi.org/10.1029/2024JC022003>
- (27) Stasko, A. B., Horrall, R. M., Hasler, A. D., & Stasko, D. (1973). Coastal Movements of Mature Fraser River Pink Salmon (*Oncorhynchus gorbuscha*) as Revealed by Ultrasonic Tracking. *Journal of the Fisheries Research Board of Canada*, 30(9), 1309–1316. <https://doi.org/10.1139/f73-211>
- (28) Tougaard, J., & Beedholm, K. (2019). Practical implementation of auditory time and frequency weighting in marine bioacoustics. *Applied Acoustics*, 145, 137–143. <https://doi.org/10.1016/j.apacoust.2018.09.022>
- (29) Vagle, S., Burnham, R., Thupaki, P., Konrad, C., Toews, S., & Thornton, S. J. (2021). Vessel presence and acoustic environment within Southern Resident Killer Whale (*Orcinus orca*) critical habitat in the Salish Sea and Swiftsure Bank area.
- (30) Veirs, V., & Veirs, S. (2005). One year of background underwater sound levels in Haro Strait, Puget Sound. *The Journal of the Acoustical Society of America*, 117(4_Supplement), 2577–2578. <https://doi.org/10.1121/1.4776892>
- (31) Veirs, S., Veirs, V., & Wood, J. D. (2016). Ship noise extends to frequencies used for echolocation by endangered killer whales. *PeerJ*, 4, e1657. <https://doi.org/10.7717/peerj.1657>
- (32) Williams, R., & Ashe, E. (2007). Killer whale evasive tactics vary with boat number. *Journal of Zoology*, 272(4), 390–397. <https://doi.org/10.1111/j.1469-7998.2006.00280.x>
- (33) Williams, R., Lusseau, D., & Hammond, P. S. (2006). Estimating relative energetic costs of human disturbance to killer whales (*Orcinus orca*). *Biological Conservation*, 133(3), 301–311. <https://doi.org/10.1016/j.biocon.2006.06.010>
- (34) Williams, R., Trites, A. W., & Bain, D. E. (2002). Behavioural responses of killer whales (*Orcinus orca*) to whale-watching boats: Opportunistic observations and experimental approaches. *Journal of Zoology*, 256(2), 255–270. Cambridge Core. <https://doi.org/10.1017/S0952836902000298>

(35) Yang, Z., Wang, T., Branch, R., & Xiao, Z. (2020). *Validation of the High-Resolution Salish Sea Tidal Hydrodynamic Model* (PNNL--30448, 1776702; p. PNNL--30448, 1776702). <https://doi.org/10.2172/1776702>